

ELECTRONIC SUPPLEMENTARY INFORMATION

**Tailoring ORR and HER electrocatalytic performances of
gold nanoparticles through metal-ligand interfaces**

David Alba-Molina,^a Alain R. Puente Santiago,^{bc} Juan J. Giner-Casares,*^a Enrique Rodríguez-Castellón,^d María T. Martín-Romero,^a Luis Camacho,^a Rafael Luque,*^{be} and Manuel Cano*^a

^a. Department of Physical Chemistry and Applied Thermodynamics, University Institute of Nanochemistry (IUNAN), University of Córdoba (UCO), Campus Universitario de Rabanales, Ed. Marie Curie, Córdoba, Spain E-14014. E-mail: jjginer@uco.es; q82calum@uco.es.

^b. Department of Organic Chemistry, IUNAN, UCO, Campus Universitario de Rabanales, Edificio Marie Curie, Córdoba, Spain E-14014. E-mail: q62alsor@uco.es.

^c. Department of Chemistry, University of Texas at El Paso, 500 W. University Avenue, El Paso, Texas 79968, United States.

^d. Department of Inorganic Chemistry, Crystallography and Mineralogy, Faculty of Sciences University of Málaga, Málaga, Spain.

^e. Peoples Friendship University of Russia (RUDN University), 6 Miklukho-Maklaya str., Moscow, Russia.

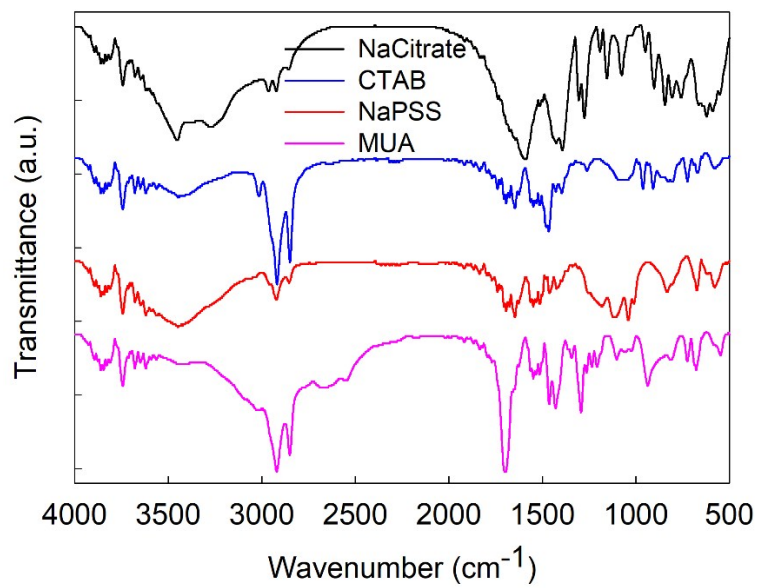


Fig. S1 FTIR spectra of the four pure ligands used in this work.

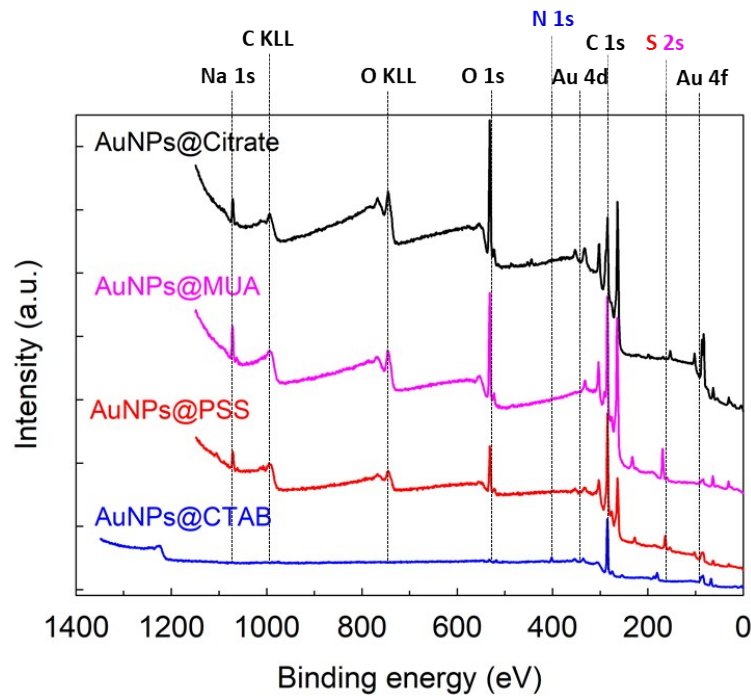


Fig. S2 XPS survey spectra of the different ligand-stabilized AuNPs on ITO supports.

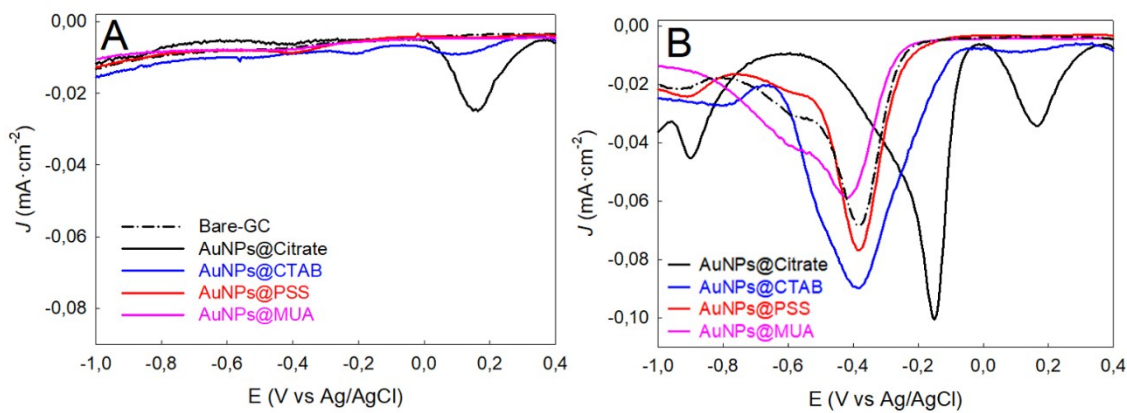


Fig. S3 DPVs curves obtained for GC electrodes modified with different ligand-stabilized AuNPs in N_2 -saturated (A) and O_2 -saturated (B) 0.5 M KOH at $0.1 \text{ V} \cdot \text{s}^{-1}$.

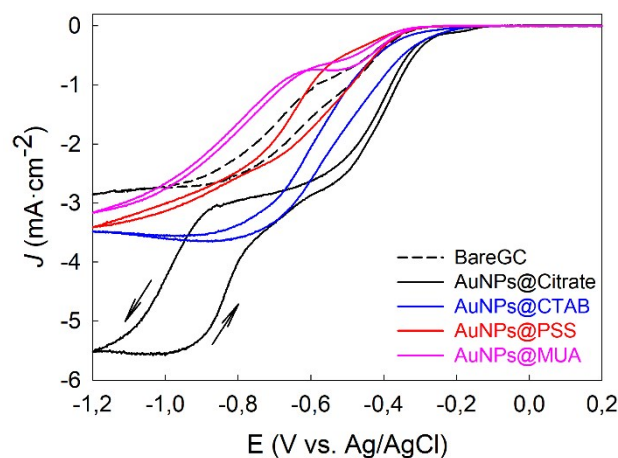


Fig. S4 Hysteresis effect during measurements with rotating disk electrode of GC electrodes modified with different ligand-stabilized AuNPs at same rotating rate of 2500 rpm. Scan rate: $10 \text{ mV} \cdot \text{s}^{-1}$.

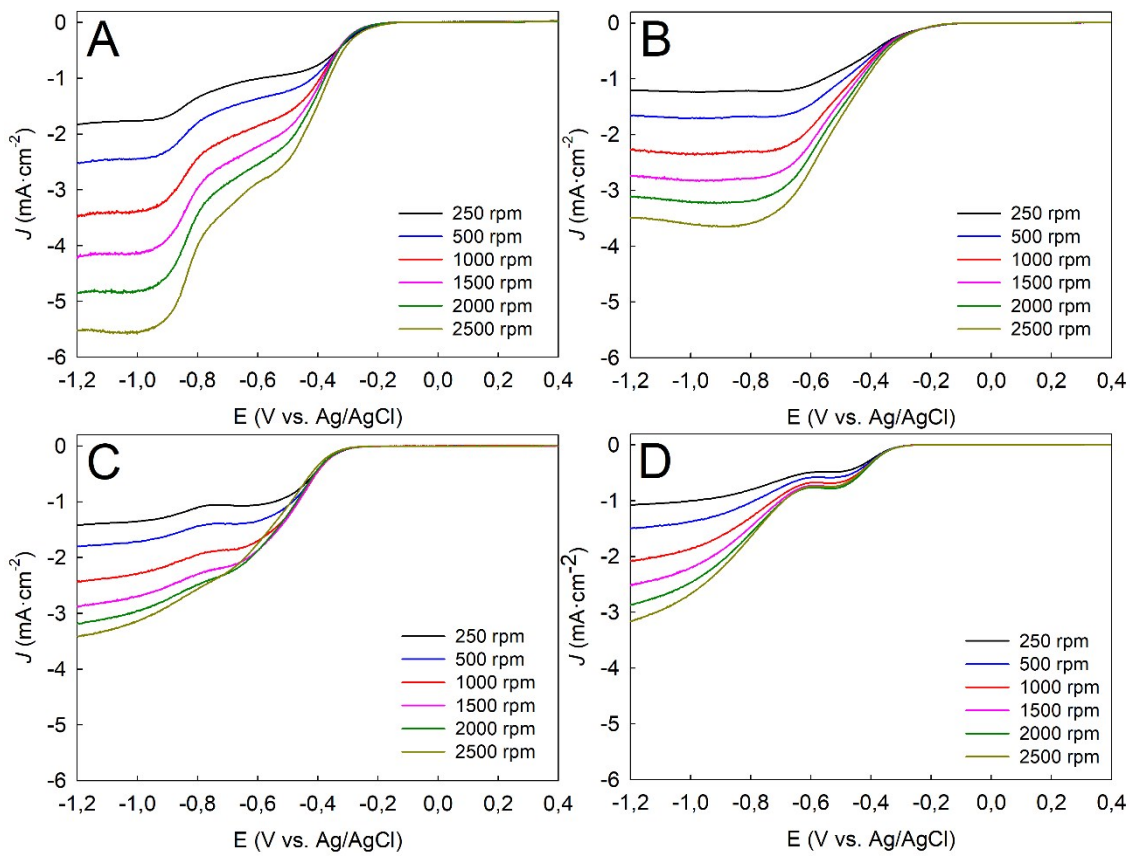


Fig. S5 Rotating-disk voltammograms for AuNPs@Citrate (A), AuNPs@CTAB (B), AuNPs@PSS (C) and AuNPs@MUA (D) modified GC electrodes at different rotation rates in O_2 -saturated 0.5 M KOH. Scan rate $10 \text{ mV}\cdot\text{s}^{-1}$.

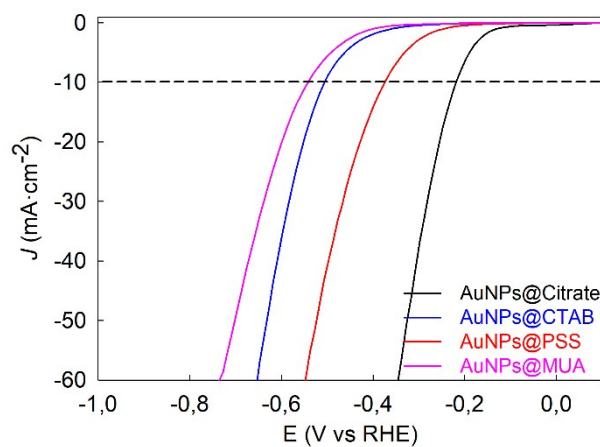


Fig. S6 Linear sweep voltammograms, without iR -correction, of GC electrodes modified with different ligand-stabilized AuNPs in N_2 -saturated 0.5 M H_2SO_4 at rotation rate of 1600 rpm. Scan rate: $2 \text{ mV}\cdot\text{s}^{-1}$.

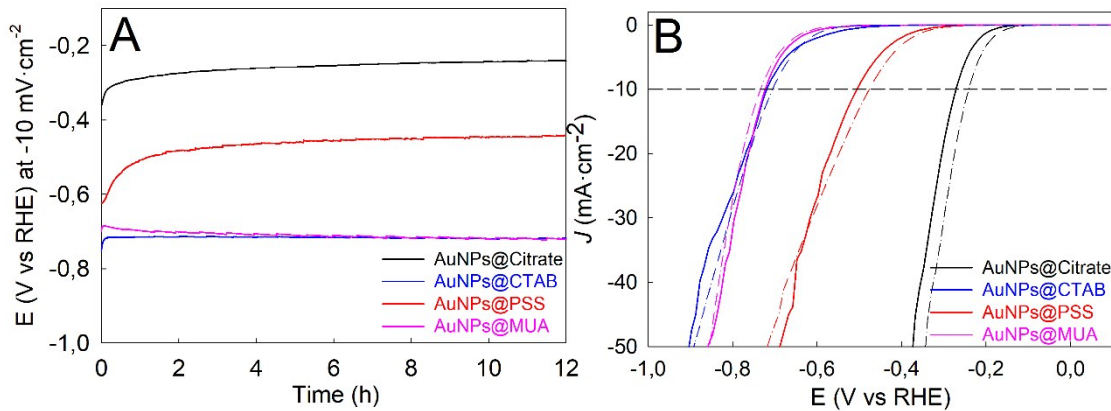


Fig. S7 (A) Chronopotentiometry measurements at $J = -10 \text{ mA} \cdot \text{cm}^{-2}$ for the different ligand-stabilized AuNPs. (B) LSV curves, without iR-correction, of the different ligand-stabilized AuNPs before (solid lines) and after (dash-dotted lines) the long-term stability test.

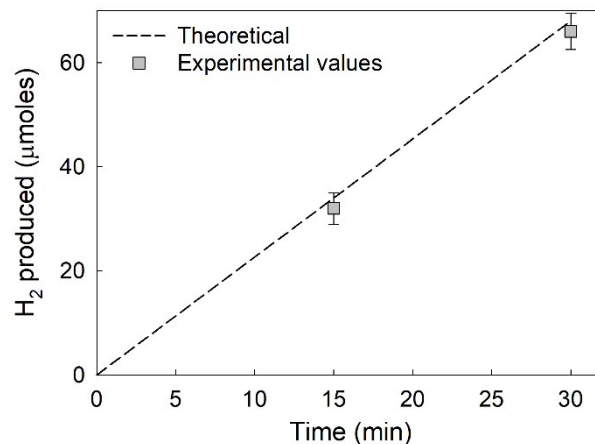


Fig. S8 Faradaic efficiency plot of AuNPs@Citrate for HER at a - 270 mV (E vs. RHE).

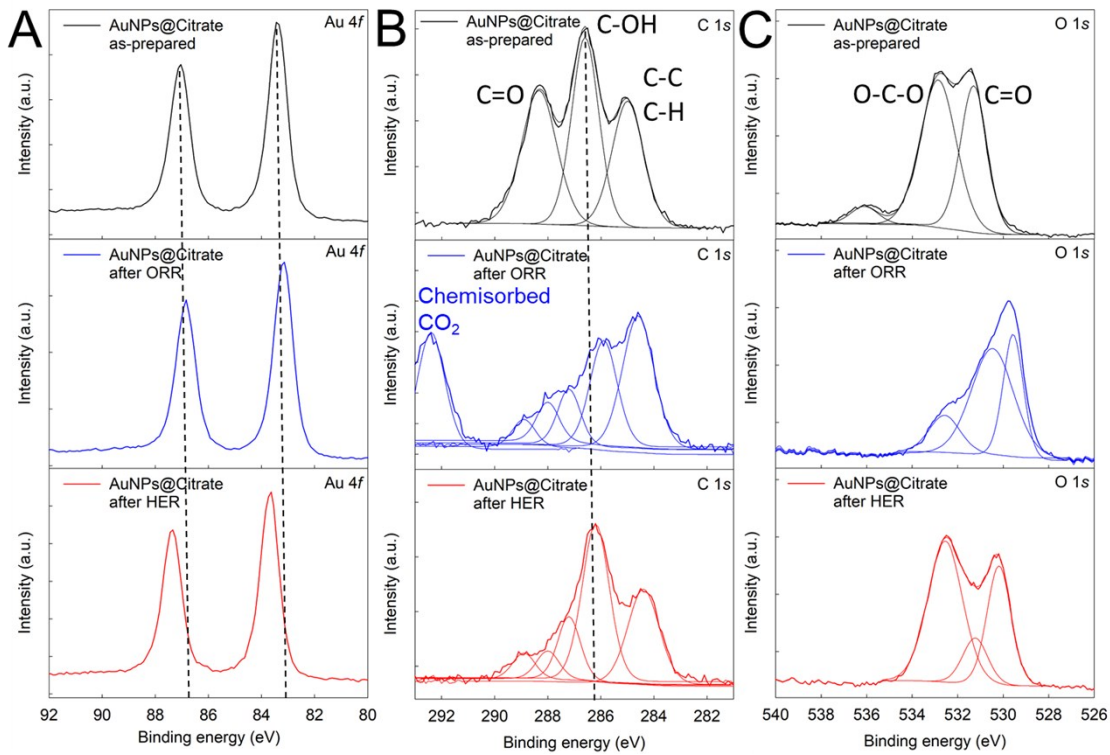


Fig. S9 High-resolution XPS spectra of Au 4f (A), C 1s (B) and O 1s (C) for AuNPs@Citrate, before and after ORR and HER measurements.

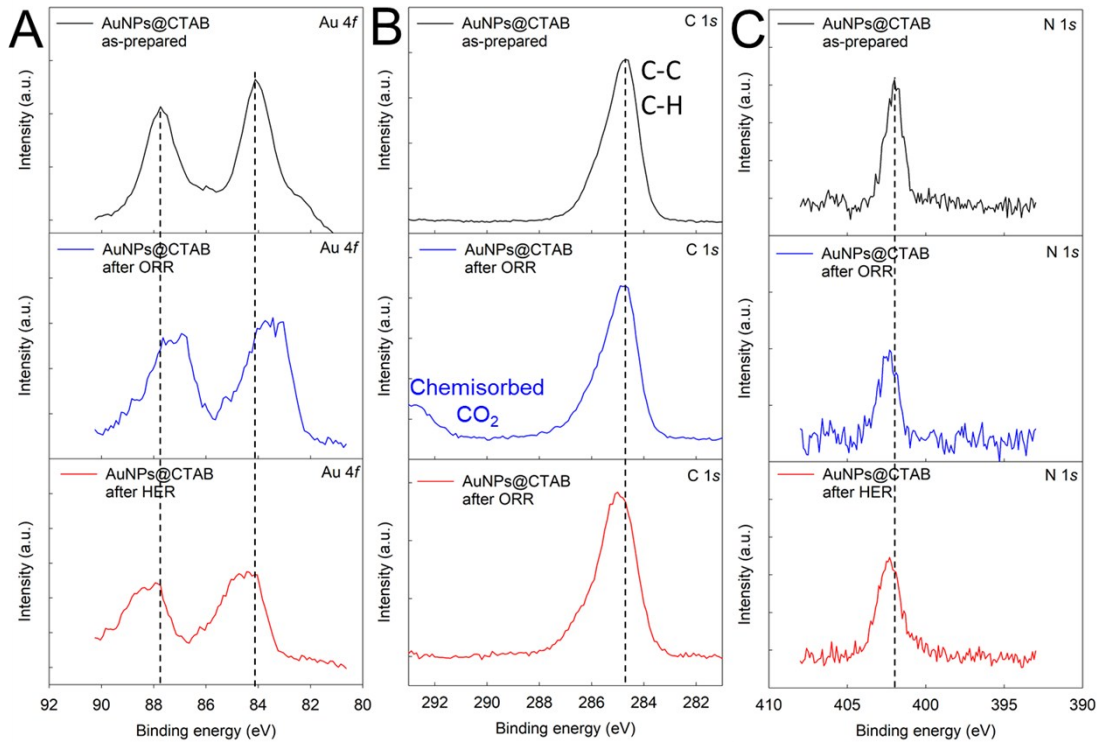


Fig. S10 High-resolution XPS spectra of Au 4f (A), C 1s (B) and N 1s (C) for AuNPs@CTAB, before and after ORR and HER measurements.

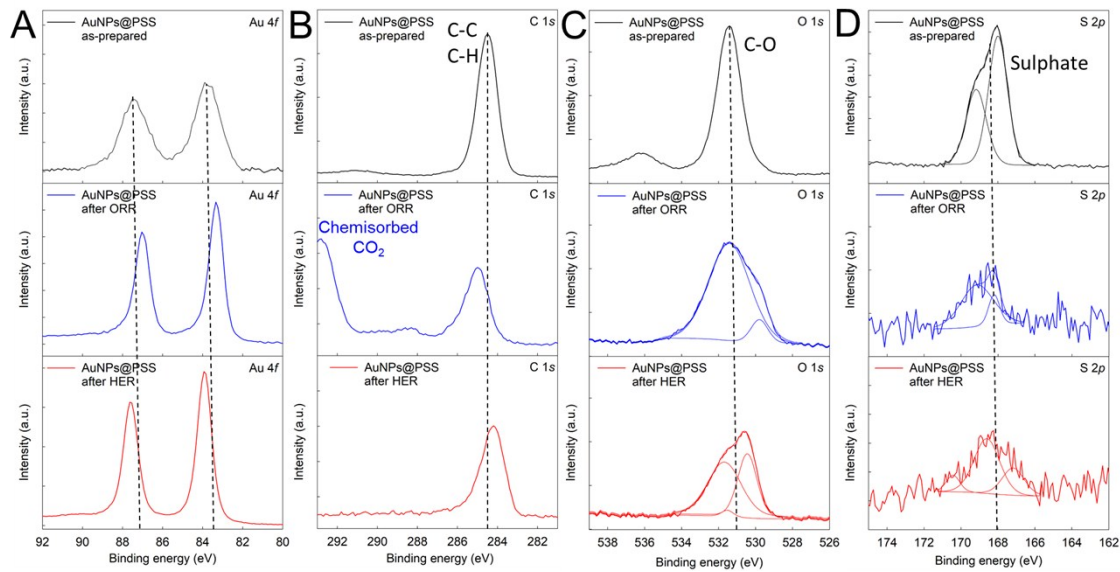


Fig. S11 High-resolution XPS spectra of Au 4f (A), C 1s (B), O 1s (C) and S 2p (D) for AuNPs@PSS, before and after ORR and HER measurements.

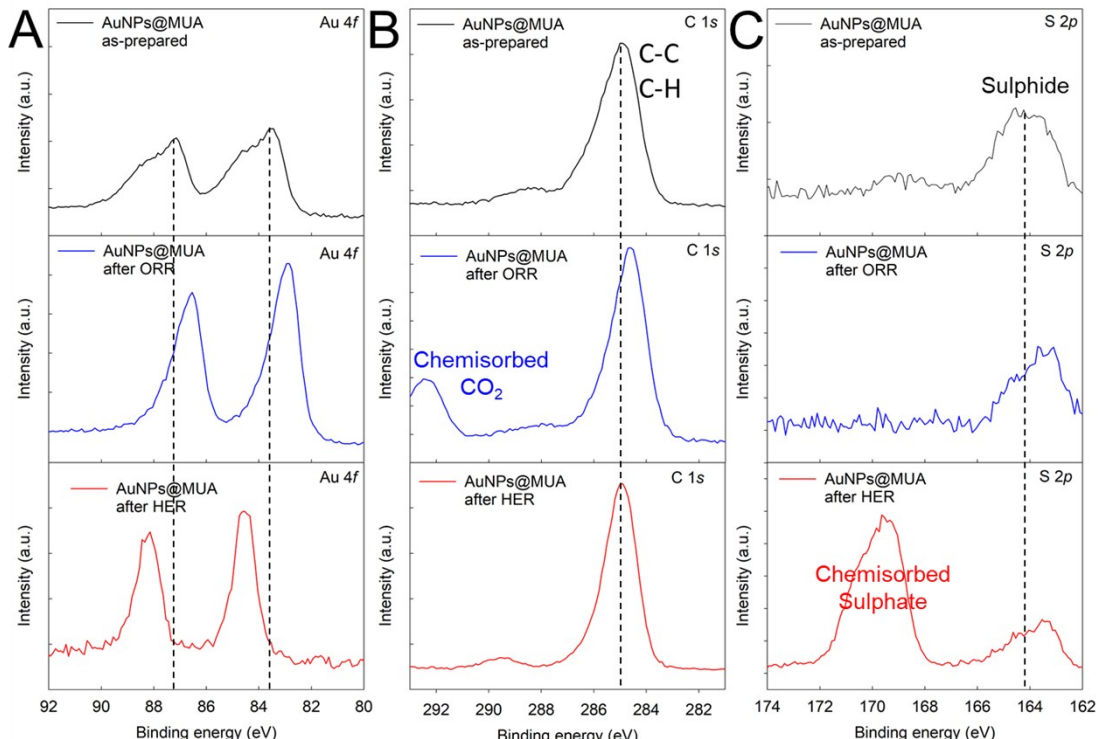


Fig. S12 High-resolution XPS spectra of Au 4f (A), C 1s (B) and S 2p (C) for AuNPs@MUA, before and after ORR and HER measurements.

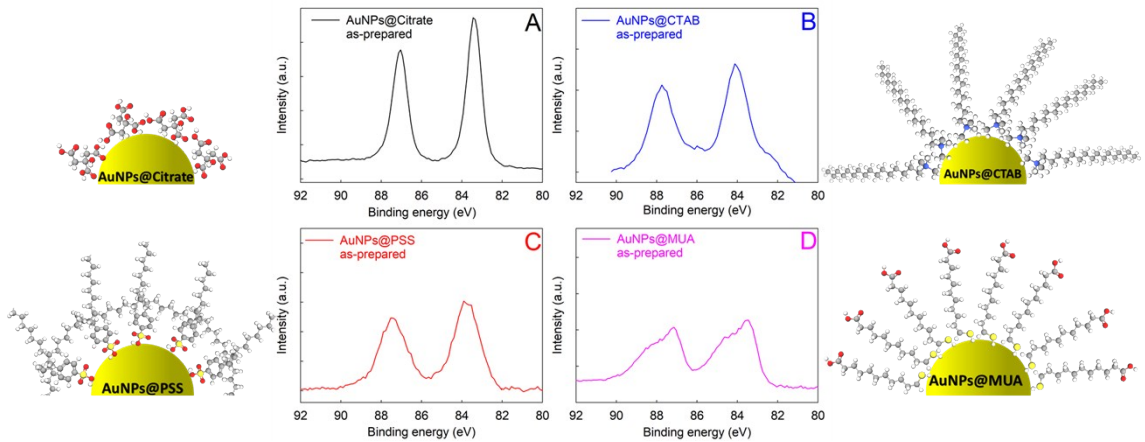


Fig. S13 High-Resolution XPS spectra of Au 4f for AuNPs@Citrate (A), AuNPs@CTAB (B), AuNPs@PSS (C) and AuNPs@MUA (D), including schematic representation of the spatial distribution of each capping ligand on AuNPs surface. Scheme is not drawn to scale.

Table S1. Summary of the ORR and HER performance of recently reported bi-functional electrocatalysts.

Catalyst ^a	Substrate	Mass density (mg/cm ²)	Reaction	η_{onset} (V)	Tafel slope (mV/dec)	$J_{\text{dif}}^{\text{b}}$ (mA/cm ²)	Overpotential	Electrolyte	Ref.
Au@Pd _{1.0}	GCE (vs RHE)	101.9	ORR	0.93	68.1	4.91	-	0.1 M KOH	S1
Au@Pd _{1.0}	GCE (vs RHE)	0.357	HER	-0.29	66.0	-	0.116 V at 20 mA/cm ²	0.5 M H ₂ SO ₄	S1
NCN-1000-5	RDE (vs RHE)	0.2	ORR	0.95	86.0	6.43	-	0.1 M KOH	S2
NCN-1000-5	RDE (vs RHE)	0.2	HER	-0.03	43.0	-	0.090 V at 10 mA/cm ²	0.5 M H ₂ SO ₄	S2
CoSAs/PTFs-600	RRDE (vs RHE)	-	ORR	0.88	57.0	6.14	-	0.1 M KOH	S3
CoSAs/PTFs-600	RRDE (vs RHE)	-	HER	-0.02	50.0	-	0.094 V at 10 mA/cm ²	0.5 M H ₂ SO ₄	S3
Co _{1-x} S/NC	RRDE (vs RHE)	0.204	ORR		70.8	-	-	0.1 M KOH	S4
Co _{1-x} S/NC	RRDE (vs RHE)	0.204	HER	-0.03	71.0	-	0.073 V at 10 mA/cm ²	0.5 M H ₂ SO ₄	S4
Mo ₂ C@NC nanomesh	RDE (vs RHE)	0.5	ORR	1.00	50.1	4.50	-	0.1 M KOH	S5
Mo ₂ C@NC nanomesh	RDE (vs RHE)	0.5	HER	-0.02	33.7	-	0.036 V at 10 mA/cm ²		S5

^aThe most proficient version of the electrocatalysts.

^bDiffusion-limiting current density.

References

- S1 J.-D. Yi, R. Xu, Q. Wu, T. Zhang, K.-T. Zang, J. Luo, Y.-L. Liang, Y.-B. Huang, R. Cao. *ACS Energy Lett.* 2018, **3**, 883-889.
- S2 Z. Zong, K. Xu, D. Li, Z. Tang, W. He, Z. Liu, X. Wang, Y. Tian. *J. Cat.* 2018, **361**, 168-176.
- S3 J.-D. Yi, R. Xu, G.-L. Chai, T. Zhang, K. Zang, B. Nan, H. Lin, Y.-L. Liang, J. Lv, J. Luo, R. Si, Y.-B. Huang, R. Cao. *J. Mater. Chem. A* 2019, **7**, 1252-1259.
- S4 J. Ding, S. Ji, H. Wang, B. G. Pollet, R. Wang. *ChemCatChem* 2019, **11**, 1026-1032.
- S5 Z. Cheng, Q. Fu, Q. Han, Y. Xiao, Y. Liang, Y. Zhao, L. Qu. *Adv. Funct. Mat.* 2018, **28**, 1705967.